The Astrophysical Journal, 805:146 (6pp), 2015 June 1 doi:10.1088/0004-637X/805/2/146

NEWLY DISCOVERED ALPHA-POOR STARS IN THE SOLAR NEIGHBORHOOD

Q. F. Xing[1,2] and G. Zhao[1]
[1] Key Laboratory of Optical Astronomy, National Astronomical Observatories, Chinese Academy of Sciences, Beijing, 100012, China; qfxing@nao.cas.cn, gzhao@nao.cas.cn
[2] University of Chinese Academy of Sciences, Beijing 100049, China
Received 2014 November 30; accepted 2015 March 19; published 2015 May 28

ABSTRACT

We present an abundance analysis for two newly discovered α-poor stars based on high-resolution spectroscopy. These stars were previously identified in the Large Sky Area Multi-Object Fiber Spectroscopic Telescope (LAMOST) Data Release 1 as candidate α-poor stars. We observed these candidate α-poor stars with the Magellan Inamori Kyocera Echelle (MIKE) spectrograph on the 6.5 m Magellan-Clay Telescope located at Las Campanas Observatory. This high-resolution analysis confirms the low [α/Fe] abundance ratios for these stars compared to those of the majority of Galactic stars with comparable metallicities ([Fe/H] ~ -0.5). The large deficiencies of α-elements suggest that these stars possess an anomalous chemical enrichment history. To have found such α-poor stars in our sample indicates that large scatters of the α-element abundance ratios may exist near solar metallicity. These results also demonstrate that our method is capable of selecting α-poor stars from low-resolution stellar spectra.

Key words: Galaxy: formation – stars: abundances – stars: atmospheres

1. INTRODUCTION

As one of the large spirals of the Local Group (LG), the Milky Way (MW) has dwarf spheroidal (dSph) satellites within its virial radius. In the past few years, the number of known dSph galaxies around the MW steadily increased with the help of the Sloan Digital Sky Survey (SDSS; York et al. 2000) and the Dark Energy Survey (Abbott et al. 2005). More than 30 dSph galaxies have been discovered as satellites of the MW (McConnachie 2012; Bechtol et al. 2015; Koposov et al. 2015). Since the MW exhibits tidal streams (e.g., Ibata et al. 2001; Bonaca et al. 2012), these dSph galaxies are believed to play some role in the formation of the MW's stellar halo. However, the available chemical abundance ratios for individual stars in classical MW dSphs show that their [α/Fe] values are significantly lower than that of the majority of Galactic halo stars (Shetrone et al. 2001; Fulbright et al. 2004; Koch et al. 2008). As the uniformity of the [α/Fe] in metal-poor Galactic halo stars has been emphasized by previous studies (e.g., Cayrel et al. 2004; Arnone et al. 2005; Lai et al. 2008), the different [α/Fe] ratios observed in MW dSphs suggest that the true building blocks of the Galactic halo must have been vastly different from the surviving dSphs (Venn et al. 2004). However, recent studies of some LG dSph galaxies (e.g., Tolstoy et al. 2009; Kirby et al. 2011, 2013) have shown that they contain a significant fraction of metal-poor stars with an enhanced α-element abundance consistent with the stellar MW halo, indicating that the dSph systems may be important contributors to the MW. Furthermore, a few extremely metal-poor stars in dSph galaxies (Frebel et al. 2010, 2014) possess similar abundance patterns of a large number of elements compared to those found in the majority of Galactic halo stars, supporting the opinion that a significant part of the outer halo originated from dSph systems.

A handful of so-called α-poor stars with abnormal [α/Fe] ratios that deviate from the trend of the halo have been found by previous works (Carney et al. 1997; King 1997; Lai et al. 2009). These anomalous metal-poor stars exhibit extremely low [α/Fe] ratios that are even below the solar value. Considering the α-deficient phenomenon found in dSph galaxies, these stars were associated with the accretion event of dSph systems. Carollo et al. (2007) suggested that the Galaxy's halo comprised inner and outer components. The outer-halo component formed through a dissipationless chaotic merging of smaller subsystems. The dSph galaxies surrounding the MW may be the surviving counterparts of such subsystems. As a significant numbers of α-poor stars have been found in several nearby dSph galaxies (e.g., Shetrone et al. 2003; Tolstoy et al. 2003), the α-poor stars found in the MW may have formed in former or present dSphs and accreted at some point. High-resolution spectroscopic studies of a population of α-poor stars (Nissen & Schuster 2010) suggested that the Galactic stars with low [α/Fe] abundance ratios originated in accreted systems. Analysis of large samples of α-poor stars will improve our understanding of the assembly history of the MW.

As the number of α-poor stars remains small, detection and analysis of large samples of such stars will provide more clues of their origin. Our previous study (Xing & Zhao 2014) presented a method to search for α-poor stars from low-resolution ($R = 2000$) SDSS stellar spectra and identified 14 candidate α-poor stars from an SDSS ninth data release (DR9) sample. Three of these candidates are confirmed to be α-poor based on high-resolution spectroscopy (Aoki et al. 2013, 2014), demonstrating that our method is capable of detecting α-poor stars from low-resolution stellar spectra. Similar methods were applied to the LAMOST (also known as Guo Shou Jing Telescope) stellar spectra with a resolving power of $R \sim 1800$ spanning 3700–9000 Å. A handful of candidate α-poor stars were identified from the LAMOST data release 1 (DR1) sample.[3] We obtained high-resolution spectroscopy with MIKE on the Magellan-Clay Telescope for several candidate α-poor stars identified by LAMOST. Two candidates are confirmed to have anomalous [Mg/Fe] ratios below the solar value. In this paper, we perform a chemical abundance analysis for two newly discovered α-poor stars from LAMOST DR1.

[3] http://dr1.lamost.org

Table 1
Observations

Object Name	R.A. (2000)	Decl. (2000)	R	Exp. (s)	S/N	RV (km s^{-1})
LAMOST J2142+0755	21:42:09.30	07:55:33.20	13.34	1200	86	24.3
LAMOST J2146+0611	21:46:30.40	06:11:16.00	11.05	450	89	8.7

Target selection and details of the observations are described in Section 2. Section 3 presents the estimation of stellar parameters and chemical abundances. Results and a discussion of the origin of our program stars are given in Section 4, as well as a brief summary of the paper.

2. OBSERVATIONS

2.1. Target Selection

The LAMOST (Zhao et al. 2012) project carried out a regular survey after a year of pilot operations. As of 2013 June, ~2 million spectra had been obtained by the LAMOST regular survey. All these spectra have been released as part of LAMOST DR1. LAMOST is a quasi-meridian reflecting Schmidt telescope (Cui et al. 2012) with an effective aperture of 4 m. The telescope is equipped with 16 spectrographs, each of which connect with 250 fibers to collect low-resolution (R = 1800) spectra over the wavelength range 3700–9000 Å. The raw data were reduced with the LAMOST standard pipeline (Luo et al. 2012), including bias subtraction, flat-fielding, cosmic-ray removal, wavelength calibration, and sky background subtraction. The stellar atmospheric parameters were determined by the ULySS (Universite de Lyon Spectroscopic analysis software) package for F-, G-, and K-type spectra with precisions of 167 K, 0.34, and 0.16 dex for $T_{\rm eff}$, log g, and [Fe/H] (Wu et al. 2011). The ULySS estimates of atmospheric parameters were also released as part of LAMOST DR1.

In order to select candidate α-poor stars from the LAMOST archive, we developed a stellar spectral matching method to estimate [Mg/Fe] ratios for low-resolution stellar spectra with atmospheric parameters in the range of $T_{\rm eff}$ = [4500, 7000] K, log g = [1.5, 5.0], and [Fe/H] = [−4, −0.5] (Xing & Zhao 2014). For given stellar spectra, we took the atmospheric parameters delivered by the LAMOST DR1 catalog as the predicted values and generated a grid of synthetic stellar spectra covering different [Mg/H] values. The [Mg/Fe] ratio was measured by searching for the best-matching synthetic spectrum over a limited wavelength range from 5000 to 5300 Å, which included the Mg I*b* lines. The synthetic stellar spectra were generated with the SPECTRUM synthesis code (Gray & Corbally 1994) based on the ATLAS9-NEWODF atmospheric models (Castelli & Kurucz 2003). After we adopted the [Mg/Fe] of the best-matching synthetic spectrum for the observed spectrum, the possible error in our determination of the [Mg/Fe] ratio was determined by quantifying the maximum abundance change introduced by errors in the adopted atmospheric parameters. Observed spectra with [Mg/Fe] ratios below −0.1 will be selected as candidate α-poor stars.

2.2. Observations and Data Reduction

For two stars identified as candidate α-poor stars from LAMOST DR1, high-resolution spectra were obtained on 2013 August 5 with the MIKE instrument (Bernstein et al. 2003) attached to the Magellan-Clay Telescope. The 0.″7 slit with 2 × 2 binning was used, yielding a resolving power of R ~ 35,000 in the blue region (3300–4900 Å) and R ~ 28,000 in the red region (4900–9400 Å), with an average signal-to-noise ratio (S/N) of 87 per pixel at 5200 Å. Basic information on the targets and the details of the high-resolution observations are listed in Table 1. The raw data were reduced using the MIKE data reduction pipeline (Kelson 2003), while the co-addition and continuum normalization were carried out with the IRAF echelle package.

3. STELLAR PARAMETERS AND ANALYSIS

The determination of stellar parameters is accomplished with a high-resolution spectroscopic analysis. We estimate effective temperatures ($T_{\rm eff}$) by demanding that the abundances of individual Fe I absorption lines are independent of their excitation potentials. Microturbulent velocities (ξ) are determined from the atomic Fe I absorption lines by ensuring that the derived abundances exhibit no trend with the reduced equivalent widths of the lines measured. Surface gravities (log g) are determined from a reasonable agreement between two ionization stages of Fe (Fe I and Fe II). The adopted values of log g are required to make the difference between the average values of Fe I and Fe II be below 0.02 dex for our program stars. Equivalent widths of selected lines are measured by fitting Gaussian profiles to the observed atomic absorption lines. An atomic line list based on data compiled by Aoki et al. (2007) and Roederer et al. (2010) is used for this analysis. The measurements of the adopted lines are listed in Table 2. In order to obtain accurate equivalent widths for spectroscopic analysis, the lines that are near the flux peaks of the echelle orders tend to be adopted. The lines near the bad-pixel regions and those that were blended with the wings of strong stellar lines were excluded. We estimate a random error of 3 mÅ in equivalent widths for our program stars based on Cayrel (1988) formalism. Table 3 shows the final adopted stellar parameters for the program stars and the parameters derived from LAMOST low-resolution spectra. The effective temperatures and surface gravities determined from high-resolution spectra are shown in Figure 1, compared with a 6 Gyr theoretical isochrone (Demarque et al. 2004) for [Fe/H] = −0.5.

The abundance estimation for individual absorption lines is performed in the standard local thermodynamic equilibrium manner, employing Kurucz's model atmospheres with no convective overshooting (Castelli & Kurucz 2003). We utilize the abundance analysis program *ABONTEST8* (developed by P. Magain) to derive abundances from the balance between equivalent widths of the observed lines and those of the theoretical model. The solar abundances from Asplund et al. (2009) are used to calculate abundance ratios [X/H] and [X/Fe] with respect to the solar abundances. The results of our abundance analysis are summarized in Table 4, including the abundance ratios relative to the solar values; the number of lines adopted for each element; the standard deviations of derived abundances of these lines; and the external uncertainties due to the variations of $T_{\rm eff}$, log g, and ξ. Since the very

Table 2
Abundance Results

Ion	λ (Å)	χ (eV)	log gf	J2142+0755 W(mÅ)	J2146+0611 W(mÅ)
Si I	4102.94	1.90	−3.140	86.5	116.0
Si I	5690.43	4.93	−1.760	22.8	16.1
Si I	5772.15	5.08	−1.750	22.1	34.4
Si I	6155.13	5.62	−0.850	29.1	56.3
Ca I	4425.44	1.88	−0.360	…	146.2
Ca I	4455.89	1.90	−0.530	108.3	125.7
Ca I	5588.76	2.52	0.358	198.2	…
Ca I	5598.49	2.52	−0.087	…	136.6
Ca I	6102.72	1.88	−0.770	104.1	122.4
Ca I	6122.22	1.89	−0.320	143.0	174.5
Mg I	4057.51	4.34	−0.890	188.6	…
Mg I	4702.99	4.34	−0.520	183.4	202.8
Mg I	5528.40	4.34	−0.500	174.6	213.5
Mg I	5711.09	4.35	−1.720	57.8	77.3
Fe I	5166.28	0.00	−4.120	…	93.7
Fe I	5171.60	1.48	−1.793	…	163.2
Fe I	5192.34	3.00	−0.420	144.7	165.0
Fe I	5194.94	1.56	−2.020	91.3	110.6
Fe I	5198.71	2.22	−2.090	66.2	84.5
Fe I	5202.34	2.18	−1.870	110.7	139.6
Fe I	5216.27	1.61	−2.080	87.8	113.8
Fe I	5217.39	3.21	−1.160	68.4	98.6
Fe I	5232.94	2.94	−0.060	173.3	…
Fe I	5254.96	0.11	−4.760	…	111.1
Fe I	5266.56	3.00	−0.390	139.2	…
Fe I	5281.79	3.04	−0.830	106.3	126.2
Fe I	5283.62	3.24	−0.520	127.0	…
Fe I	5324.18	3.21	−0.100	157.6	…
Fe I	5332.91	1.56	−2.940	…	85.2
Fe I	5371.49	0.96	−1.640	193.3	…
Fe I	5397.13	0.92	−1.980	142.1	179.2
Fe I	5405.77	0.99	−1.850	138.1	…
Fe I	5415.20	4.39	0.640	104.9	144.4
Fe I	5434.52	1.01	−2.130	126.0	149.4
Fe I	5506.78	0.99	−2.797	96.2	110.3
Fe I	5576.10	3.43	−1.000	…	86.8
Fe I	5586.76	3.37	−0.140	145.9	188.3
Fe I	6065.48	2.61	−1.410	96.6	105.0
Fe I	6136.61	2.45	−1.410	70.1	…
Fe I	6137.69	2.59	−1.350	89.9	…
Fe I	6219.28	2.20	−2.450	59.6	79.4
Fe I	6230.72	2.56	−1.280	109.5	130.1
Fe I	6252.56	2.40	−1.690	80.7	106.8
Fe I	6393.60	2.43	−1.580	99.4	110.1
Fe I	6421.35	2.28	−2.010	79.0	100.6
Fe I	6430.85	2.18	−1.950	82.1	102.1
Fe I	6494.98	2.40	−1.240	113.2	…
Fe I	6677.99	2.69	−1.420	92.1	110.9
Fe II	4233.17	2.58	−2.000	97.7	115.6
Fe II	4583.83	2.80	−2.020	99.6	107.8
Fe II	4923.93	2.89	−1.320	…	178.1
Fe II	5018.45	2.89	−1.220	172.8	182.3
Fe II	5234.63	3.22	−2.180	60.8	74.8
Fe II	5534.85	3.24	−2.865	38.7	…
Fe II	6247.56	3.89	−2.435	39.8	…
Fe II	6432.68	2.89	−3.501	23.6	…
Fe II	6456.38	3.90	−2.185	43.9	…

strong lines are inappropriate for precision abundance determinations, the Si and Mg abundances are determined from relatively weak lines, excluding the Si I 3905 Å line and the Mg triplet lines at 5167, 5172, and 5183 Å. We present the line-to-line scatter errors for elements analyzed in this work in Table 4. The agreement of the derived abundances of each element from the individual absorption lines is fairly good. We select candidate α-poor stars from low-resolution LAMOST stellar spectra by searching the best-matching synthetic spectrum to the Mg I*b* lines of the observed spectrum. Our estimates of [Mg/Fe] from low-resolution spectra are in good agreement with the results in this analysis (differences within 0.15 dex for both of our stars). Figure 2 shows the results of spectral matching for the Mg I*b* lines of the low-resolution spectra for LAMOST J2142+0755 and J2146+0611. Figure 3 exhibits the comparison of synthetic spectra for the Mg I 5528 and 5711 Å lines of the high-resolution spectra for LAMOST J2142+0755 and J2146+0611.

Table 3
Adopted Stellar Parameters

Object Name	High Resolution				Low Resolution		
	$T_{\rm eff}$	log g	[Fe/H]	ξ	$T_{\rm eff}$	log g	[Fe/H]
LAMOST J2142+0755	5950	4.6	−0.53	0.8	5834	4.3	−0.56
LAMOST J2146+0611	5400	3.7	−0.49	0.9	5371	3.3	−0.73

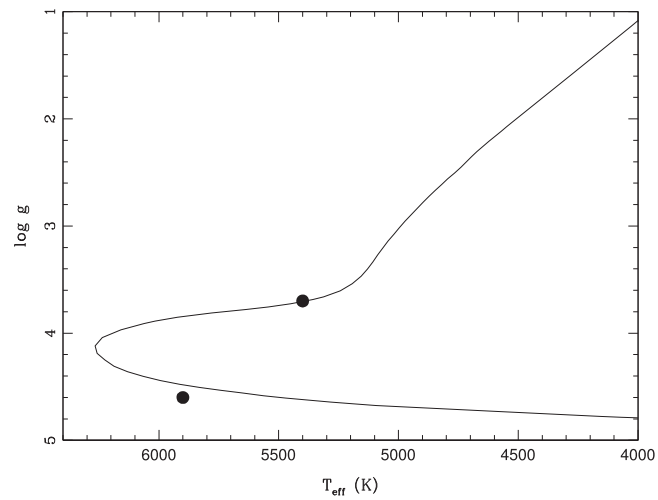

Figure 1. Adopted $T_{\rm eff}$ vs. log g shown for the program stars. Overplotted is the 6 Gyr theoretical isochrone with [Fe/H] = −0.5 from Demarque et al. (2004).

4. RESULTS AND DISCUSSION

In Figure 4, we compare the α-abundances of LAMOST J2142+0755 and J2146+0611 to the published results of a large sample of Galactic stars from the literature compiled by Venn et al. (2004) and Bensby et al. (2014). The observed ratios of [Mg/Fe] in LAMOST J2142+0755 and J2146+0611 are much lower than that of the vast majority of Galactic stars with comparable metallicities. These subsolar (below the solar ratio) [Mg/Fe] ratios had not been seen at [Fe/H] ~ -0.5 in the Galaxy before. High-precision analyses of large samples of stars in the thin and thick disks of the Galaxy have demonstrated that the trend of the α-element abundance versus [Fe/H] is distinctly different between the various Galactic components (Bensby et al. 2004; Reddy et al. 2006). The thin and thick disks exhibit a clearly distinct abundance with [Fe/H]

Table 4
Abundance Results

Ion	J2142+0755			J2146+0611			$\Delta T_{\rm eff}$	$\Delta \log\ g$	$\Delta\xi$
	[X/Fe]	σ	N	[X/Fe]	σ	N	($\pm 100\ K$)	(± 0.5 dex)	(± 0.5 km s^{-1})
[Fe I/H]	−0.53	0.03	29	−0.49	0.05	25	±0.07	∓0.08	∓0.06
[Fe II/H]	−0.53	0.04	8	−0.50	0.04	5	±0.00	±0.03	∓0.04
Mg I	−0.21	0.10	4	−0.16	0.05	3	±0.05	∓0.06	∓0.03
Si I	−0.06	0.12	4	+0.07	0.03	4	±0.03	±0.04	∓0.02
Ca I	+0.09	0.08	4	+0.08	0.04	5	±0.08	∓0.09	∓0.04

Note. σ represents the line-to-line scatter.

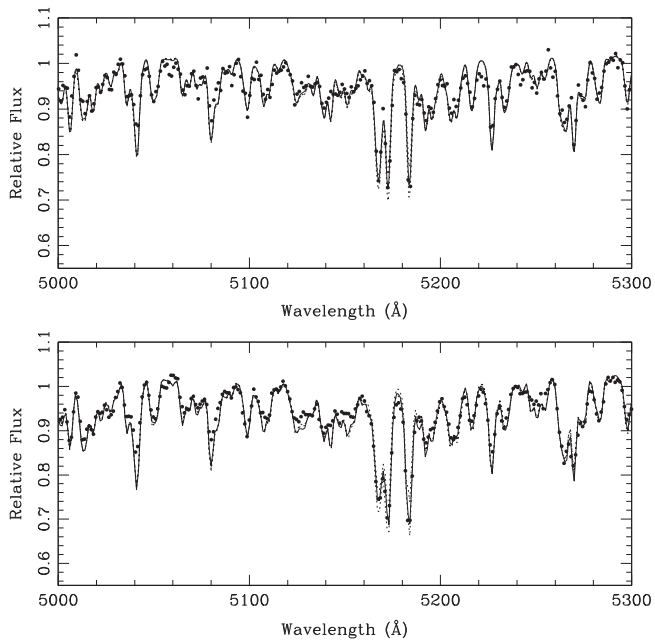

Figure 2. Dots represent the low-resolution observed spectra of J2142+0755 (upper panel) and J2146+0611 (lower panel). The solid black lines are the best-matching synthetic spectra for J2142+0755 with parameters ($T_{\rm eff}$, log g, [Fe/H], [Mg/Fe]) = (5834 K, 4.3, −0.56, −0.2) and J2146+0611 with parameters ($T_{\rm eff}$, log g, [Fe/H], [Mg/Fe]) = (5371 K, 3.3, −0.73, −0.3). The short dashed lines correspond to synthetic spectra with changes of ±0.15 dex in [Mg/H].

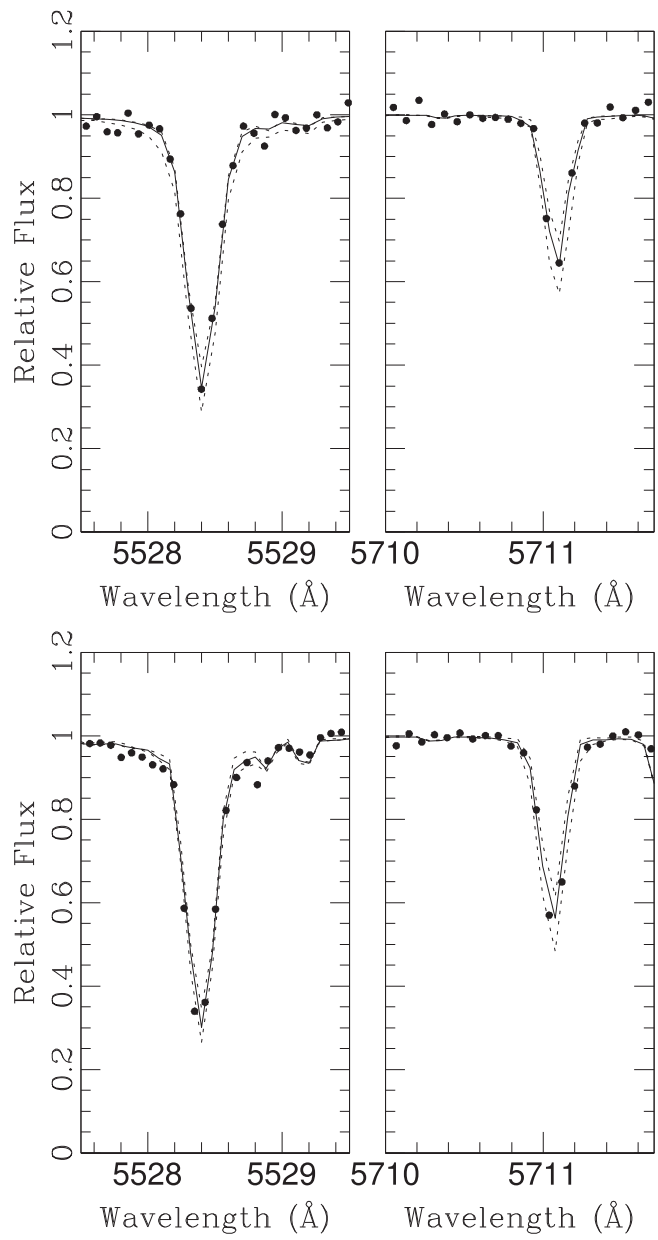

Figure 3. Mg I 5528 and 5711 Å lines of the high-resolution spectra for J2142+0755 (upper panels) and J2146+0611 (lower panels) shown as black dots. The synthetic spectra for J2142+0755 with parameters ($T_{\rm eff}$, log g, [Fe/H], [Mg/Fe]) = (5950 K, 4.6, −0.53, −0.21) and J2146+0611 with parameters ($T_{\rm eff}$, log g, [Fe/H], [Mg/Fe]) = (5400 K, 3.7, −0.49, −0.16) are shown as solid black lines. The short dashed lines correspond to synthetic spectra with changes of ±0.15 dex in [Mg/H].

<0. The observed thick disk stars possess an enhanced α-element abundance ([Mg/Fe] $\sim$ 0.3–0.4) for metallicities below [Fe/H]~ -0.4, where the trend of [α/Fe] ratios begins to decline toward solar values. The thin disk [α/Fe] trend smoothly declines to solar values at [Fe/H] ~ 0 from a slight α-enhancement ([Mg/Fe] $\sim$ 0.1–0.2). There exists no obvious "knee" in the [Mg/Fe] trend for the thin disk stars (Bensby et al. 2003), suggesting a lower star formation rate (McWilliam 1997).

Subsolar [Mg/Fe] with [Fe/H] < -0.4 have been uncovered in a few intermediately metal-poor halo field stars, with abnormally low [Mg/Fe] ratios that are more than 0.4 dex below the expected values for Galactic halo stars of comparable metallicities (Ivans et al. 2003). Stephens & Boesgaard (2002) suggest such α-poor stars are components of the outer halo while Cohen et al. (2007) suggest that the standard SN II models should be modified to find explosion parameters that can reproduce the properties derived from the peculiar metal-poor stars. Similar α-poor stars have been discovered in a few nearby MW dSph galaxies (Sbordone et al. 2007; Koch

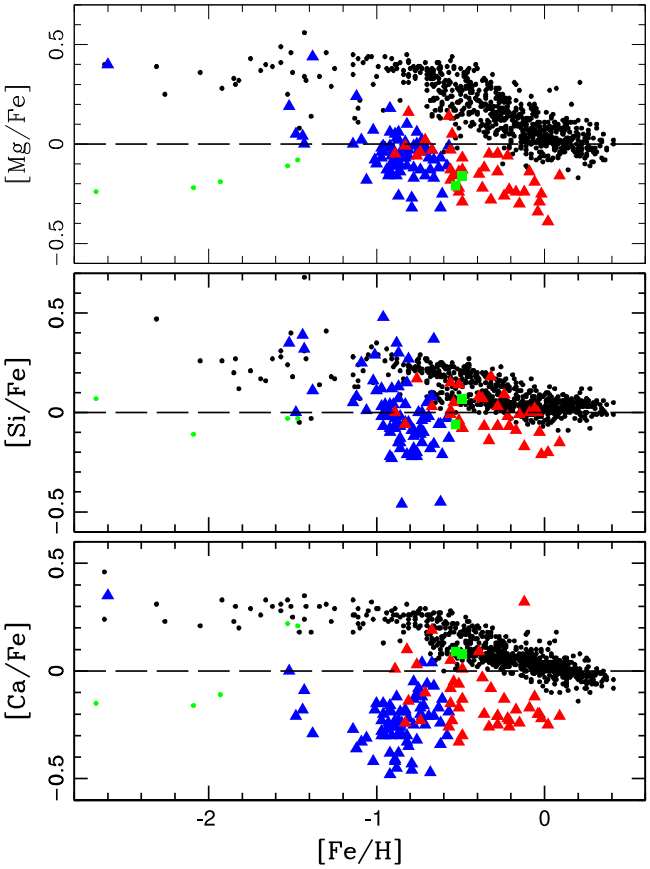

Figure 4. Abundance ratios of α-abundances as a function of [Fe/H]. Our candidates are shown as green squares and nearby dSph stars from the comparison sample (Monaco et al. 2007; Sbordone et al. 2007; Letarte et al. 2010; Tafelmeyer et al. 2010; McWilliam et al. 2013) are in colored triangles: Fornax (blue), Sgr (red). The abundances of other Galactic stars (Venn et al. 2004; Bensby et al. 2014) are plotted with black filled circles. The abundances of known α-poor metal-poor stars (King 1997; Ivans et al. 2003; Cohen et al. 2013) are plotted with green filled circles.

et al. 2008; Shetrone et al. 2009). According to the scenario given by Nissen et al. (2014), α-poor stars may have been accreted from dSph galaxies with a relatively slow chemical evolution. Recently, three newly discovered α-poor stars with subsolar [Mg/Fe] ratios have been found by Cohen et al. (2013), suggesting that these α-poor stars should be studied as a new population of Galactic metal-poor stars. Although our program stars are significantly metal-rich compared to the currently known metal-poor α-poor stars, the existing explanations of their origin may also be suitable for LAMOST J2142+0755 and J2146+0611.

Stars associated with Sgr have been confirmed to be α-poor in the metallicity range of $-1.0 \leqslant$ [Fe/H] $\leqslant +0.0$ (McWilliam & Smecker-Hane 2005; Sbordone et al. 2007). Sbordone et al. (2007) find subsolar [Mg/Fe] ratios for 12 Sgr stars. McWilliam et al. (2013) perform a chemical abundance analysis for three stars in the Sgr dSph galaxies, discovering that they all possess [Mg/Fe] ratios that are below the solar value. The unusually low α-abundances are also seen in other dSph galaxies. Shetrone et al. (2001) performed high-resolution spectral analyses for a sample of stars in Draco, Ursa Minor, and Sextans dSph galaxies. In these dSph galaxies, the [α/Fe] ratios appear to be lower than that of the Galactic stars with comparable metallicities. The same pattern has also been observed in Sculptor, Fornax, Carina, and Leo I with the UV-Visual Echelle Spectrograph (Shetrone et al. 2003; Tolstoy et al. 2003). The α-deficiency is now a common phenomenon in the dSph satellites of the Galaxy. Tissera et al. (2012) suggested that more massive dSph satellites typically have lower [α/Fe] ratios. In contrast, a significant fraction of stars with high α-abundances are suggested to be contained in less luminous dSph galaxies (Starkenburg et al. 2013). These α-deficiencies demonstrated by LAMOST J2142+0755 and J2146+0611 suggest that they may share a common explanation for their anomalous abundance patterns with the α-poor stars in the dSph satellites of the Galaxy. Figure 4 shows a comparison of the α-abundance ratios found in our program stars with that of stars in nearby dSph galaxies, such as Fornax (Letarte et al. 2010; Tafelmeyer et al. 2010) and Sgr (Monaco et al. 2007; Sbordone et al. 2007; McWilliam et al. 2013). LAMOST J2142+0755 and J2146+0611 exhibit subsolar [Mg/Fe] ratios that are nearly 0.3 dex below the typical values for Galactic stars with comparable metallicities. Since their α-abundances are similar to those of stars in MW dSph galaxies, they may originate from regions that were significantly deficient in massive stars in former or current dSph systems. The environments that were deficient in massive stars will lead to intrinsic scatter in the [α/Fe] ratios and abnormal [α/Fe] ratios (Vargas et al. 2013). We performed a kinematic analysis following Fuhrmann (1998), which suggested that the stars with $V_{\rm total} > 180$ km s^{-1} belong to the halo. Two program stars are classified as disk stars based on their space velocities. Their disk-like kinematics do not seem to suggest that they are signatures of accretion of present-day dSph galaxies. Several simulations (Martínez-Delgado et al. 2007; Purcell et al. 2011) showed the Sgr tidal stream falling onto the Galactic disk, crossing the proximity of the Sun. We next see how well the two stars match observational studies (Johnston et al. 1995; Majewski 2004) and theoretical models (Law & Majewski 2010) of the Sgr stream. The locations and velocities of our program stars do not appear to be consistent with simulations of the infall of the Sgr dSph galaxy and the observational data of stars identified as likely stream members. Our program stars are not likely to be stellar debris in the Sgr stream. They may have originated from former dSph systems that were already merged into the MW at some time in the past.

We discovered two α-poor stars in the solar neighborhood based on high-resolution abundance analysis. Although the present results suggest that our program stars may have originated from environments that were deficient in massive stars, the origin and the occurrence frequency of such α-poor stars remain unclear. Discoveries of more α-poor stars will improve our understanding of their nature and the formation of the MW.

We are grateful to the referee for providing very helpful comments on our manuscript. This study is supported by the National Natural Science Foundation of China under grant Nos. 11390371, 11233004, 11303040, and U1431106. The Guoshoujing Telescope (the Large Sky Area Multi-Object Fiber Spectroscopic Telescope (LAMOST)) is a National Major Scientific Project built by the Chinese Academy of Sciences. Funding for the project has been provided by the National Development and Reform Commission. LAMOST is operated and managed by the National Astronomical Observatories, Chinese Academy of Sciences.

REFERENCES

Abbott, T., Aldering, G., Barlow, M., et al. 2005, arXiv:astro-ph/0510346
Aoki, W., Beers, T. C., Lee, Y. S., et al. 2013, AJ, 145, 13
Aoki, W., Honda, S., Beers, C., et al. 2007, ApJ, 660, 747
Aoki, W., Tominaga, N., Beers, T. C., et al. 2014, Sci, 345, 912
Arnone, E., Ryan, S. G., Argast, D., Norris, J. E., & Beers, T. C. 2005, A&A, 430, 507
Asplund, M., Grevesse, N., Sauval, A. J., & Scott, P. 2009, ARA&A, 47, 481
Bechtol, K., Drlica-Wagner, A., Balbinot, E., et al. 2015, ApJ, submitted (arXiv:1503.02584)
Bensby, T., Feltzing, S., & Lundström, I. 2003, A&A, 410, 527
Bensby, T., Feltzing, S., & Lundström, I. 2004, A&A, 415, 155
Bensby, T., Feltzing, S., & Oey, M. S. 2014, A&A, 562, A71
Bernstein, R., Shectman, S. A., Gunnels, S. M., et al. 2003, Proc. SPIE, 4841, 1694
Bonaca, A., Geha, M., & Kallivayalil, N. 2012, ApJ, 760, 6
Carney, B. W., Wright, J. S., Sneden, C., et al. 1997, AJ, 114, 363
Carollo, D., Beers, T. C., Lee, Y. S., et al. 2007, Natur, 450, 1020
Castelli, F., & Kurucz, R. L. 2003, IAU Symp. 210, Modelling of Stellar Atmospheres, ed. N. Piskunov, W. W. Weiss, & D. F. Gray (San Francisco, CA: ASP), A20
Cayrel, R., Depagne, E., Spite, M., et al. 2004, A&A, 416, 1117
Cayrel, R. 1988, in IAU Symp. 132, The Impact of Very High S/Ns Spectroscopy on Stellar Physics, ed. G. Cayrel de Strobel, & M. Spite (Dordrecht: Kluwer), 345
Cohen, J. G., McWilliam, A., Christlieb, N., et al. 2007, ApJL, 659, L161
Cohen, J. G., Christlieb, N., Thompson, I., et al. 2013, ApJ, 778, 56
Cui, X.-Q., Zhao, Y.-H., Chu, Y.-Q., et al. 2012, RAA, 12, 1197
Demarque, P., Woo, J.-H., Kim, Y.-C., & Yi, S. K. 2004, ApJS, 155, 667
Frebel, A., Simon, J. D., Geha, M., & Willman, B. 2010, ApJ, 708, 560
Frebel, A., Simon, J. D., & Kirby, E. N. 2014, ApJ, 786, 74
Fuhrmann, K. 1998, A&A, 338, 161
Fulbright, J. P., Rich, R. M., & Castro, S. 2004, ApJ, 612, 447
Gray, R. O., & Corbally, C. J. 1994, AJ, 107, 742
Ibata, R., Irwin, M., Lewis, G. F., & Stolte, A. 2001, ApJ, 547, 133
Ivans, I. I., Sneden, C., James, C. R., et al. 2003, ApJ, 592, 906
Johnston, K. V., Spergel, D. N., & Hernquist, L. 1995, ApJ, 451, 598
Kelson, D. D. 2003, PASP, 115, 688
King, J. R. 1997, AJ, 113, 2302
Kirby, E. N., Cohen, J. G., Guhathakurta, P., et al. 2013, ApJ, 779, 102
Kirby, E. N., Cohen, J. G., Smith, G. H., et al. 2011, ApJ, 727, 79
Koch, A., Grebel, E. K., Gilmore, G. F., et al. 2008, AJ, 135, 1580
Koposov, S. E., Belokurov, V., Torrealba, G., & Evans, N. W. 2015, ApJ, in press (arXiv:1503.02079)
Lai, D. K., Bolte, M., Johnson, J. A., et al. 2008, ApJ, 681, 1524
Lai, D. K., Rockosi, C. M., Bolte, M., et al. 2009, ApJ, 697, 63
Law, D., & Majewski, S. 2010, ApJ, 714, 229
Letarte, B., Hill, V., Tolstoy, E., et al. 2010, A&A, 523, A17
Luo, A.-L., Zhang, H.-T., Zhao, Y.-H., et al. 2012, RAA, 12, 1243
Majewski, S. R., Kunkel, W. E., Law, D. R., et al. 2004, AJ, 128, 245
Martínez-Delgado, D., Peñarrubia, J., Jurić, M., Alfaro, E. J., & Ivezić, Z. 2007, ApJ, 660, 1264
McConnachie, A. W. 2012, AJ, 144, 4
McWilliam, A. 1997, ARA&A, 35, 503
McWilliam, A., & Smecker-Hane, T. A. 2005, ApJ, 622, L29
McWilliam, A., Wallerstein, G., & Mottini, M. 2013, ApJ, 778, 149
Monaco, L., Bellazzini, M., Bonifacio, P., et al. 2007, A&A, 464, 201
Nissen, P. E., Chen, Y. Q., Carigi, L., Schuster, W. J., & Zhao, G. 2014, A&A, 568, 25
Nissen, P. E., & Schuster, W. J. 2010, A&A, 511, 10
Purcell, C. W., Bullock, J. S., Tollerud, E. J., et al. 2011, Natur, 477, 301
Reddy, B. E., Tomkin, J., Lambert, D. L., & Allende Prieto, C. 2006, MNRAS, 367, 1329
Roederer, I. U., Sneden, C., Thompson, I. B., et al. 2010, ApJ, 711, 573
Sbordone, L., Bonifacio, P., Buonanno, R., et al. 2007, A&A, 465, 815
Shetrone, M. D., Côté, P., & Sargent, W. L. W. 2001, ApJ, 548, 592
Shetrone, M. D., Venn, K. A., Tolstoy, E., et al. 2003, AJ, 125, 684
Shetrone, M. D., Siegel, M. H., Cook, D. O., & Bosler, T. 2009, AJ, 137, 62
Starkenburg, E., Helmi, A., de Lucia, G., et al. 2013, MNRAS, 429, 725
Stephens, A., & Boesgaard, A. M. 2002, AJ, 123, 1647
Tafelmeyer, M., Jablonka, P., Hill, V., et al. 2010, A&A, 524, A58
Tissera, P. B., White, S. D. M., & Scannapieco, C. 2012, MNRAS, 420, 255
Tolstoy, E., Hill, V., & Tosi, M. 2009, ARA&A, 47, 371
Tolstoy, E., Venn, K. A., Shetrone, M. D., et al. 2003, AJ, 125, 707
Vargas, L. C., Geha, M., Kirby, E. N., & Simon, J. D. 2013, ApJ, 767, 134
Venn, K. A., Irwin, M., Shetrone, M. D., et al. 2004, AJ, 128, 1177
Wu, Y., Luo, A., Li, H., et al. 2011, RAA, 11, 924
Xing, Q. F., & Zhao, G. 2014, ApJ, 790, 33
York, D. G., Adelman, J., Anderson, J. E. Jr., et al. 2000, AJ, 120, 1579
Zhao, G., Zhao, Y.-H., Chu, Y.-Q., Jing, Y.-P., & Deng, L.-C. 2012, RAA, 12, 723